PLANT SCIENCE TODAY
Vol 13(2): 1-10
https://doi.org/10.14719/pst.13051

eISSN 2348-1900

RESEARCH ARTICLE

Biogenic zinc nanoparticles synthesized from *Terminalia chebula* Retz: A sustainable approach to synthesis, characterization and antimicrobial studies

Aakanksha Sharma[1], Neha Behar[2] & Rupal Purena[1*]

[1]Department of Applied Science, Shri Rawatpura Sarkar University, Raipur 493 661, Chhattisgarh, India
[2]Department of Biotechnology, D.L.S. P.G. College, Bilaspur 495 001, Chhattisgarh, India

*Correspondence email - drrupal4786@gmail.com, dr.rupalpurena@sruraipur.ac.in

Received: 03 December 2025; Accepted: 14 February 2026; Available online: Version 1.0: 19 March 2026; Version 2.0: 01 April 2026

Cite this article: Aakanksha S, Neha B, Rupal P. Biogenic zinc nanoparticles synthesized from *Terminalia chebula* Retz: A sustainable approach to synthesis, characterization and antimicrobial studies. Plant Science Today. 2026; 13(2): 1-10. https://doi.org/10.14719/pst.13051

Abstract

Zinc nanoparticles (ZnNPs) are particularly valuable due to their broad applications, including antibacterial, antifungal, anti-diabetic and wound healing properties. In this study the phytochemicals of *Terminalia chebula* Retz. fruits were extracted via Soxhlet extraction and cold extraction method using methanol as solvent after that, ZnNPs were synthesized using a green chemistry methodology employing the above methanolic extracts. After the synthesis, qualitative phytochemical analysis of the extract was executed to precisely identify the key biomolecules responsible for facilitating the nanoparticle formation. The ZnNPs were characterized using UV-Visible (UV-Vis) spectroscopy, Fourier transform infrared spectroscopy (FTIR), X-ray diffraction (XRD) and scanning electron microscopy (SEM). Subsequently, their effectiveness as an antibacterial agent was tested against Gram-positive and Gram-negative bacteria. Visual observation confirmed nanoparticles formation through a colour change from brown to creamy. UV-Vis spectroscopy showed characteristic absorption peak around 360–380 nm, which is the typical excitonic peak of Zn nanoparticles. X-ray diffraction analysis confirmed the highly crystalline and polycrystalline nature of the zinc nanoparticles, while FTIR spectra revealed differences in extraction efficiency between Soxhlet and cold extraction methods. Scanning electron microscopy analysis showed irregular morphology and agglomerated clusters of the synthesized ZnNPs. Crucially, the *T. chebula* mediated ZnNPs demonstrated broad-spectrum antimicrobial activity, often surpassing streptomycin, with optimal activity between 150–200 µg/mL, highlighting its potential as a source for natural antimicrobial compounds.

Keywords: characterizations; green synthesis; nanoparticles; *Terminalia chebula* fruits

Introduction

Nanotechnology is an innovative field poised to revolutionize various scientific disciplines. At its core, nanotechnology involves nanoparticles atomic or molecular clusters smaller than 100 nm. Nanoparticles are essentially modified versions of basic elements; these nanoparticles are created by altering their atomic and molecular structures. The unique physiochemical properties, that significantly differ from their larger, "bulk" counterparts, making them attractive for diverse applications (1).

Zinc nanoparticles (ZnNPs) are particularly interesting due to their broad applications, including antibacterial, antifungal, anti-diabetic, anti-inflammatory, wound healing, antioxidant and optical uses. Because traditional methods for producing these nanoparticles often rely on toxic chemicals and harsh conditions, researchers are now turning to greener approaches (2). Green synthesis methods are gaining popularity because they are good for the environment. Green synthesis uses living things like bacteria, plants and fungi to create nanoparticles. This approach reduces environmental damage and makes the nanoparticles safer for medical uses due to improved biocompatibility (3).

Plant-mediated nanoparticle biosynthesis follows a three-stage process: reduction, growth and stabilization. The reduction phase is key point here; specific plant biomolecules act as reducing agents, converting metal ions from their original salt forms into neutral metal atoms. This initiates the nucleation of these atoms. Then, in the growth phase, these newly formed metal atoms coalesce to create nanoparticles, often accompanied by further reduction of metal ions. While this growth boosts the nanoparticles' stability, it's important to control nucleation to prevent aggregation and maintain desired shapes. The final stage is stabilization, where plant metabolites attach to the nanoparticles, giving them their most favourable and stable structure (4).

Terminalia chebula Retz., also known as Haritaki, is a fruit-bearing tree from South Asia and a staple in traditional Indian Ayurvedic medicine. It is a member of the Combretaceae family, is widely recognized in Ayurvedic medicine. *Terminalia chebula* are rich in compounds like tannins, flavonoids and phenolic compounds. These compounds make *T. chebula* useful in creating nanoparticles, where it can act as both a stabilizer and a reducing agent (5).

Terminalia chebula is valued for its diverse therapeutic properties, including benefits for heart health, antimicrobial action, antioxidant effects, anti-diabetic activity, improved gastrointestinal motility and wound healing (6).

This study aimed to achieve three main goals: first, to synthesize ZnNPs from both the Soxhlet and cold methanolic extracts of *T. chebula* fruits and its qualitative phytochemical analysis; second, to analyze the characteristics of these synthesized ZnNPs using techniques like UV–Visible spectroscopy, Fourier transform infrared spectroscopy (FTIR), X-ray diffraction (XRD) and scanning electron microscopy (SEM); and third, to evaluate their antibacterial ability against both Gram-positive and Gram-negative bacteria.

Materials and Methods

Materials

Zinc nitrate hexahydrate $Zn(NO3)_2{\cdot}6H2O$ Molecular weight 297.48 g/mol and purity > 98.0%), sodium hydroxide pellets NaOH Molecular weight 40 g/mol, were acquired from Hi Media. *Terminalia chebula* fruits were collected from June to October 2023 from 2 locations in Madhya Pradesh, India: Dumar-Kachhar (Lat 23.175727, Long 82.136303) and Kotma (Lat 23.171587, Long 82.126507). Only well-matured, healthy and dried fruits were selected. All other reagents were of analytical grade and used as received.

Preparation of the fruit extracts

Two distinct methodologies were employed for extract preparation from *T. chebula* fruits: Soxhlet extraction and cold maceration method. For Soxhlet extraction, 20 g of finely powdered *T. chebula* was placed in a thimble within the apparatus. Methanol was used as the solvent, undergoing continuous vaporization, condensation and siphoning cycles for 48 hr to ensure comprehensive analyte removal, as this technique is known to thermodynamically enhance extraction efficiency compared to simple soaking methods. The resulting methanolic extract was then concentrated under reduced pressure. In parallel, the cold maceration process, recognized for its effectiveness in isolating bioactive compounds like phenolics, flavonoids and tannins from *Terminalia* species, was also utilized. In this method, dried *T. chebula* fruits were oven-dried (50–65 °C for 20–40 min), pulverized and then 20 g of the powder was steeped in 150 mL of methanol. This mixture was heated in a water bath for 7–8 hr, cooled to room temperature and subsequently filtered using Whatman filter paper No. 1. The filtered extract was stored at 4 °C and used for nanoparticle synthesis within a week (7). The extracts were concentrated by evaporating the solvent until a solid or semi-solid mass was obtained. The concentrated extract was weighed to calculate the percentage yield and then stored in 4 °C for phytochemical analysis and antibacterial activity study (8).

$$\text{Percentage Yield} = \frac{\text{Weight of extract}}{\text{Weight of powdered plant sample}} \times 100$$

Synthesis of zinc nanoparticles

Zinc nanoparticles were synthesized using a green method involving *T. chebula* dried fruit extract. The 30 mL of the previously prepared fruit extract was heated to 60 °C and 5 g of zinc nitrate hexahydrate was added. The mixture was continuously stirred at 60 °C for one hour until it transformed into a yellowish paste. This temperature was crucial, yielding the optimal number of nanoparticles. The resulting paste was then calcined in a furnace at 40 °C for 2 hr. The remaining powder was thoroughly washed multiple times with methanol and distilled water, followed by drying at 100 °C to yield the ZnNPs ready for characterisation (6).

Phytochemical analysis

The phytochemical analysis was conducted to identify the potential phytochemicals present in the fruit extract that may be responsible for its bioactivity. The extracts underwent chemical analysis to identify the presence of various bioactive compounds, including alkaloids analysis (Mayer's test, Wagner's test, Hager's test), flavonoids analysis (alkaline reagent test), phenols analysis (Ferric chloride test), carbohydrates analysis (Molisch's test, Fehling's test, Benedict's test) glycosides analysis (Keller- Killiani test, Legal's Test), terpenoids analysis, saponins analysis (foam test), proteins analysis (Xanthoprotein test, Precipitation test) and tannins analysis. This phytochemical analysis was conducted using established biochemical reaction methods (9, 10).

Characterisation

Visual observation

Confirmation of synthesized ZnNPS was done by a visible shift in the synthesizing solution's colour to cream (11).

UV-Visible spectroscopy

UV-Visible spectroscopy (Labtronics, Model-29) using de-ionized water as a blank was employed to characterize the Zn nanoparticles, the presence of Zn ions was confirmed at an absorption peak between 360–380 nm with an detection range of 200–800 nm (11, 12).

Fourier transform infrared spectroscopy (FTIR)

Fourier transform infrared spectroscopy (Thermo Scientific, Nicole iS5) was employed to analyse the functional groups present in both synthesized ZnNPs. All the samples were mixed properly with 100 mg KBr and properly grounded before analysis. The analysis of functional groups in both the extract and the synthesized Zn-NPs was conducted within the spectral range of 500 to 4000 cm^{-1} (13).

Scanning electron microscopy (SEM)

Scanning electron microscopy was done at SAIF- STIC Cochin, India to examine the morphology and size of a sample (14).

X-ray diffraction (XRD)

X-ray diffraction analysis was done at SAIF STIC- Cochin, India. X-Ray Diffraction is employed to ascertain the crystalline nature and structural characteristics of synthesized zinc nanoparticles (15).

Antimicrobial activity

The ZnNPs synthesized using *T. chebula* fruit extract was tested for antimicrobial activity by standard agar well-diffusion method against different microorganisms which include *Escherichia coli* (MTCC 443), *Staphylococcus pyogenes* (MTCC 442), *Pseudomonas aeruginosa* (MTCC 424), *Xanthomonas oryzae* (MTCC 11107) (16). The pure cultures of microorganisms were sub-cultured on Nutrient agar medium. The 100 µL of fresh overnight grown cultures of the microorganism were transferred into fresh sterile nutrient broth medium and grown at 37 °C for 4–9 hr. The inoculum was adjusted to 1 x 10^8 CFU/mL through spectrophotometer at 620 nm. The 0.08 absorbance value was taken to standardize the inoculum. The inoculums were dispersed on Mueller Hinton agar plates. Each strain swabbed consistently using sterile cotton swabs. Wells of 6 mm diameter were formed

on agar using gel puncture and varying concentration of AgNPs solution (50–250 µg/mL) along with positive (50–250 µg/mL) and negative control was placed in the wells. After incubation at 37 °C for 24 hr, the varied levels of zone of inhibition were assessed.

Statistical analysis

Statistical methodology is essential for the comprehensive assessment of antimicrobial efficacy within diverse research settings. The antibacterial assay was conducted in triplicate and all results are expressed as the mean ± standard deviation (SD). Statistical validation was performed using one-way analysis of variance (ANOVA) to compare the mean values across different treatments. Significant differences between means were determined and compared using R software, with a *p*-value of less than 0.05 considered statistically significant.

Results and Discussion

Percentage yield of fruit extracts

The percentage yield obtained for Soxhlet and cold extract was 4.8 % and 4.6 % respectively. The percentage yield of the extracts is affected by many factors such as solvent used, the method of extraction, sample particle size (coarsely grounded or finely powdered form), presence of interfering substances, sample to solvent volume ratio, extraction time and temperature (8). These results agree with other studies (17).

Phytochemical analysis

Qualitative phytochemical screening of the *T. chebula* fruit extracts prepared using Soxhlet and cold methanolic extraction procedures revealed the presence of alkaloids, flavonoids, saponins and tannins in both extracts. Nevertheless, phytosterols and terpenoids were not present in the cold extract and were only found in the Soxhlet extract. The presence of these phytochemicals, particularly tannins, flavonoids and terpenoids, plays a critical role in the bio-reduction of zinc ions and the consequent stability of biosynthesized zinc nanoparticles. The higher phytochemical diversity in the Soxhlet extract may contribute to enhanced reduction efficiency and improved capping ability during nanoparticle formation.

Characterization of Zn nanoparticle

Visual observation

Terminalia chebula fruit extract, naturally brown due to phytochemicals like tannins and flavonoids, is used to synthesise ZnNPs. These phytochemicals play a crucial role by reducing zinc ions from a precursor into elemental zinc, thereby generating the nanoparticles. The most apparent sign of this successful transformation is the solution's colour changing from brown to a creamy hue (Fig. 1).

UV-Visible (UV-Vis) spectroscopy

UV-Visible spectroscopy confirmed the successful synthesis of ZnNPs using both Soxhlet and cold extracts of *T. chebula*. The UV spectrum exhibited a characteristic absorption peak around 360–380 nm, which is the typical excitonic peak of ZnNPs. The presence of this peak confirms the successful formation of Zn NPs, (Fig. 2). In both synthesized nanoparticles (TCZnS and TCZnC), Zinc nanoparticles synthesized from Soxhlet extract and cold extract of *T. chebula* respectively, the broad UV-Vis spectra, particularly the high absorbance below 400 nm, indicated the significant role of organic compounds from the respective *T. chebula* extracts in reducing zinc ions and stabilizing the formed nanoparticles. One of the study shows that the calcination of samples at 50 °C and 70 °C causes the strong absorption maximum of ZnNPs, typically below 400 nm (18). Another study also discussed that UV-Vis spectroscopy of Zn nanoparticles, with an absorption peak at 357 nm indicating the intrinsic band-gap of Zn-absorption (19). One more study showed ZnNPs show a strong absorption band at approximately 355 nm, with an excitonic absorption peak at about 258 nm, which is significantly lower than the material's band gap wavelength of 358 nm (20).

X-ray diffraction (XRD) analysis

The X-ray diffraction pattern obtained for TCZnS which represents zinc nanoparticles synthesized using *T. chebula* fruit Soxhlet extract, showed crucial insights into their structural properties.

A key observation from the XRD graph is the crystalline nature of the synthesized zinc nanoparticles. This is evidenced by the presence of numerous sharp and clearly defined peaks throughout the diffraction spectrum (Fig. 3A). Importantly, the

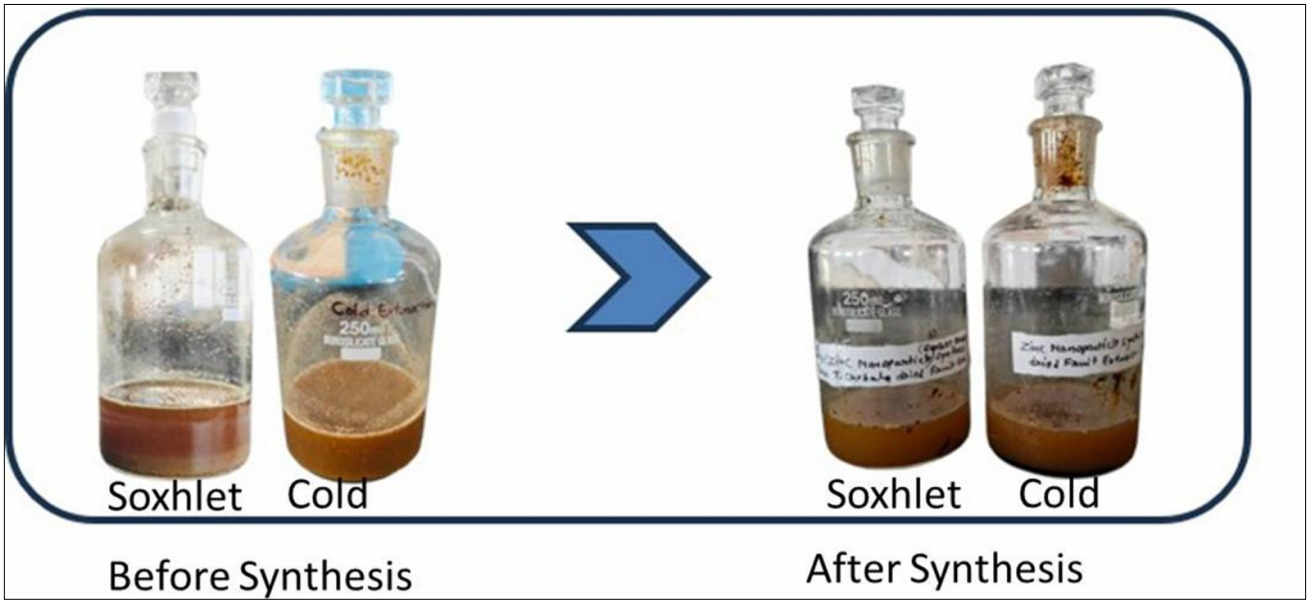

Fig. 1. Analysis of visual observation of *Terminalia chebula* Soxhlet and cold methanolic extract mediated- synthesis of zinc nanoparticles.

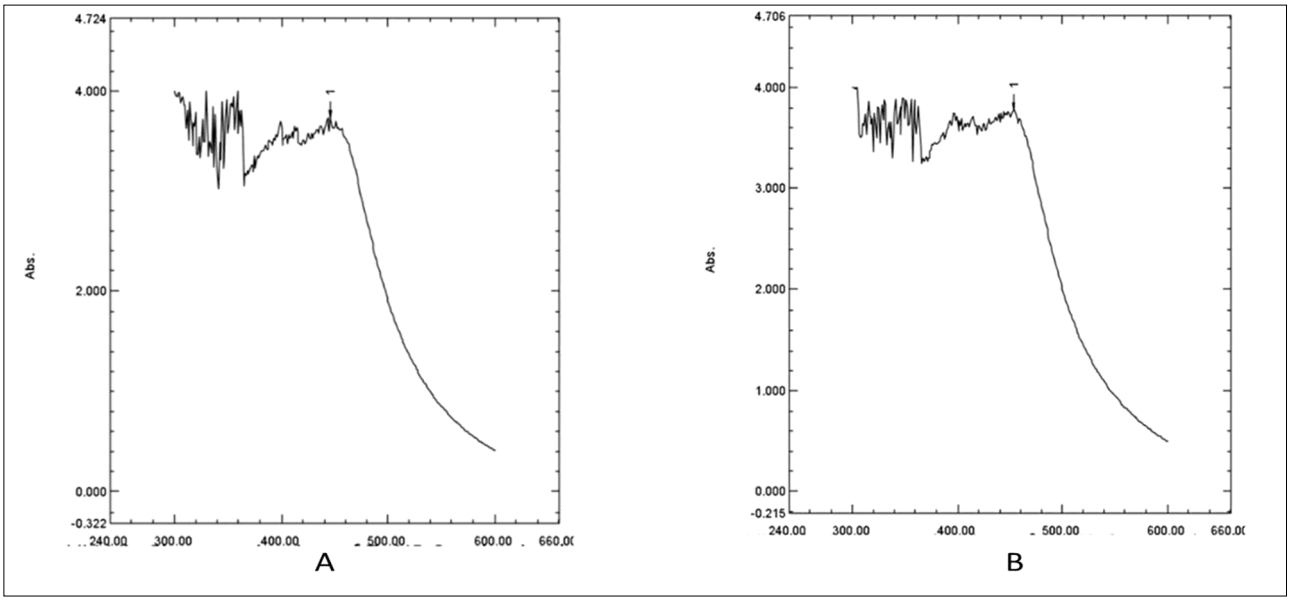

Fig. 2. UV-Vis spectra of *Terminalia chebula* mediated zinc nanoparticles. A: TCznS; B: TCZnC.

TCZnS: *Terminalia chebula* Soxhlet extract mediated zinc nanoparticles; TCZnC: *Terminalia chebula* cold extract mediated zinc nanoparticles.

absence of any broad, diffuse humps confirms that the material is predominantly crystalline, lacking any significant amorphous regions. Among these peaks, a particularly strong and distinct reflection is noted at approximately 2θ = 28.287°. This dominant peak suggests that a specific crystallographic plane is highly ordered and abundant, or that there's a preferred direction in which the nanoparticles grew.

Furthermore, the existence of several other well-resolved peaks at distinct 2θ values, specifically around 9.677°, 12.336°, 13.607°, 17.539°, 21.562°, 24.076°, 26.208°, 29.984°, 32.246° and 37.565°, indicates that the material is polycrystalline. This means the sample is composed of numerous small crystallites that are oriented in various directions. The sharpness and high intensity of all these peaks further underscore the good crystallinity and suggest that the nanoparticles possess either relatively large crystallite sizes or a very well- formed crystal lattice. XRD analysis of TCZnS revealed an average crystallite size of ~42–58 nm. Additionally, the low and flat background noise in the diffraction pattern speaks to the purity of the sample and the quality of the measurement.

The XRD pattern presented for the "TCZnC" sample, likely zinc nanoparticles synthesized with *T. chebula* fruit cold extract, offers clear insights into its structural characteristics. The pattern reveals the material to be highly crystalline, as evidenced by the distinct presence of numerous sharp and intense diffraction peaks (Fig. 3B). The absence of a broad, amorphous hump further confirms that the sample is almost entirely crystalline, with no significant non-crystalline components.

A standout feature of the pattern is a remarkably prominent and sharp diffraction peak observed at approximately 2θ=28.462°. The high intensity of this peak suggests either a strong preferred orientation in the material's crystal growth or the high abundance of a specific crystallographic plane within its structure. Beyond this dominant peak, several other well-defined reflections are apparent at various 2θ values, including roughly 9.688°, 12.363°, 13.675°, 17.558°, 20.781°, 24.232°, 25.419°, 32.389°, 37.660° and 46.660°. These multiple peaks collectively confirm that the synthesized material possesses a polycrystalline structure,

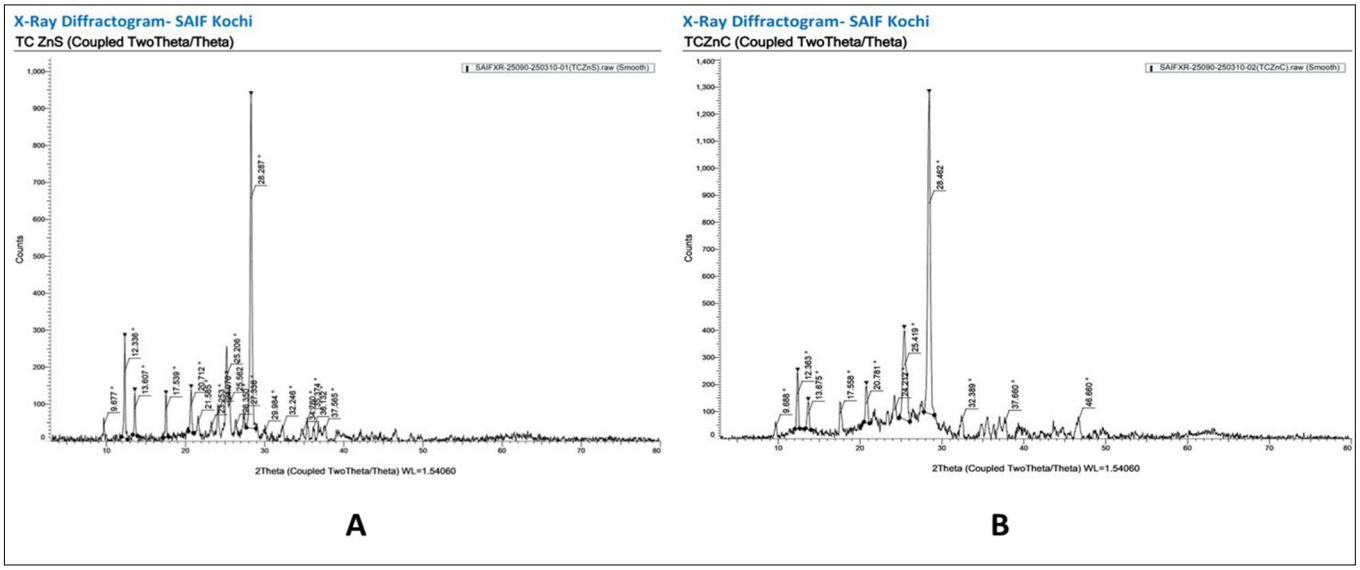

Fig. 3. X-ray diffraction of *Terminalia chebula* mediated zinc nanoparticles. A: TCznS; B: TCZnC.

TCZnS: *Terminalia chebula* Soxhlet extract mediated zinc nanoparticles; TCZnC: *Terminalia chebula* cold extract mediated zinc nanoparticles.

indicating it is composed of numerous small, randomly oriented crystalline grains. The narrowness and high intensity of these peaks collectively imply excellent crystallinity and possibly larger crystallite sizes, or at the very least, a well-formed and ordered crystal lattice. XRD analysis of TCZnC revealed an average crystallite size of ~15–32.8 nm. Furthermore, the low and consistent background noise in the XRD pattern suggests a clean sample and high-quality data acquisition. It's also worth noting that if this "TCZnC" sample is related to "TCZnS" from prior analyses, minor shifts in peak positions (for instance, the primary peak here being at 28.462° compared to 28.287° in previous graphs) could point to subtle differences in lattice parameters, internal stress, or even a variation in crystalline phase or composition, despite the overall diffraction pattern appearing similar (Fig. 3).

The X-ray Diffraction data clearly demonstrates the successful synthesis of highly crystalline zinc-based nanoparticles, specifically designated as TCZnS and TCZnC. The presence of sharp and intense diffraction peaks in both analyses provides robust evidence of a well-ordered internal structure and confirms their polycrystalline nature. While a prominent reflection was observed at approximately 2θ≈28.287° for TCZnS and 2θ≈28.462° for TCZnC, highlighting a dominant crystallographic plane, a precise identification of the specific crystalline phase such as zinc oxide would necessitate a comprehensive comparison of these observed peak positions against established standard crystallographic databases like JCPDS (Joint Committee on Powder Diffraction Standards) or ICDD (International Centre for Diffraction Data) cards. Furthermore, it is highly probable that the *T. chebula* fruit extract, a natural biological agent, played a significant and vital role as both a reducing and stabilizing agent during the formation and stabilization of these crystalline nanoparticles (21). In one study researchers thoroughly analysed nanoparticles synthesized differently, all nanoparticle types exhibit very similar, highly crystalline structures with prominent, sharp peaks. This suggests that the synthesis method had little impact on crystalline arrangement (22).

Fourier transform infrared spectroscopy (FTIR) analysis

Fourier transform infrared (FTIR) analysis of ZnNPs synthesized from *T. chebula* fruit extracts, obtained through both Soxhlet (TCZnS) and cold extract (TCZnC) reveals a striking similarity in their overall chemical profiles (Fig. 4). Both spectra exhibit characteristic broad absorption bands for hydroxyl groups (~3300 cm^{-1}), indicating the presence of alcohols, phenols, or carboxylic acids. Similarly, distinct peaks around ~2900 cm^{-1} point to aliphatic C-H stretching, while prominent bands between~1600–1650 cm^{-1}suggest carbonyl and aromatic C=C stretching, typical of phenolic compounds, flavonoids, or quinones.

Despite the general similarities, subtle differences in the FTIR spectra suggest variations in extraction efficiency or the concentration of specific compounds. The TCZnS spectrum generally displays sharper and more intense absorption bands, particularly in the~1600 cm^{-1} and ~2900 cm^{-1} regions, compared to the TCZnC spectrum. These observations imply that the Soxhlet extraction method, benefiting from continuous solvent cycling and elevated temperatures, might lead to a higher concentration of certain compounds or a more efficient extraction of specific constituents.

In previous study, FT-IR spectroscopy of green-synthesized Zn nanoparticles also revealed several characteristic peaks at 3455, 1640, 1400, 1070.1, 960 and 846 cm^{-1} (23). Other studies also

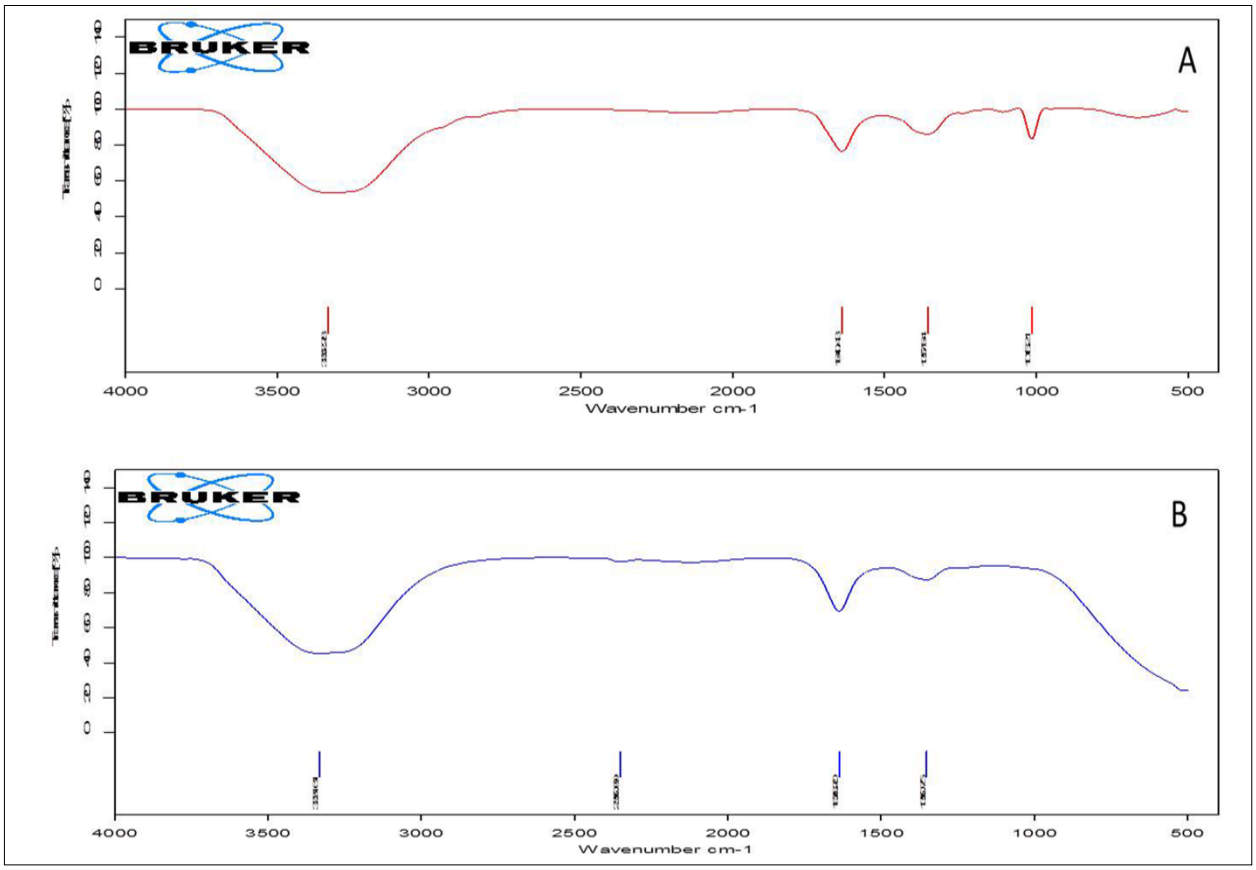

Fig. 4. Fourier transform infrared spectra of *Terminalia chebula* mediated Zinc nanoparticles. A:TCznS; B: TCZnC.

TCZnS: *Terminalia chebula* Soxhlet extract mediated zinc nanoparticles; TCZnC: *Terminalia chebula* cold extract mediated zinc nanoparticles.

reported that FT-IR analysis for ZnNPs showed characteristic flexing vibrations at 448.6 cm^{-1}, C-O stretching at 1026.6 cm^{-1}, hydroxyl groups at 1358.2 cm^{-1} and C-H stretching at 2889.1 cm^{-1} (24, 25).

Scanning electron microscopy (SEM) analysis

This frequently used approach effectively determines the crystallinity, structural surface morphology, size, size distribution, shape and dispersion of high-resolution ZnNPs (26). The SEM analysis consistently shows that the ZnNPs are irregular in shape and significantly agglomerated across all magnifications, rather than being discrete particles (Fig. 5 and 6). The particles exhibit a wide size range, from potentially nanometer-scale particles to larger aggregates. At lower magnifications (X500, X1,500), the images reveal a broad overview of extensive material accumulation with a rough, granular texture and distinct clusters. Higher magnifications (X3,500, X7,000) provide more detail, highlighting the irregular morphology and porous nature of larger aggregates. The highest magnification images (X7,000), including one with measurement markings, indicate the presence of particles likely ranging from nanometers to micrometers, confirming attempts to quantify the dimensions of these irregular, clustered structures.

The SEM analysis showed that the ZnNPs synthesized from *T. chebula* dried fruit cold extract (TCZnC), exhibit an irregular morphology, showing both individual particles and agglomerated

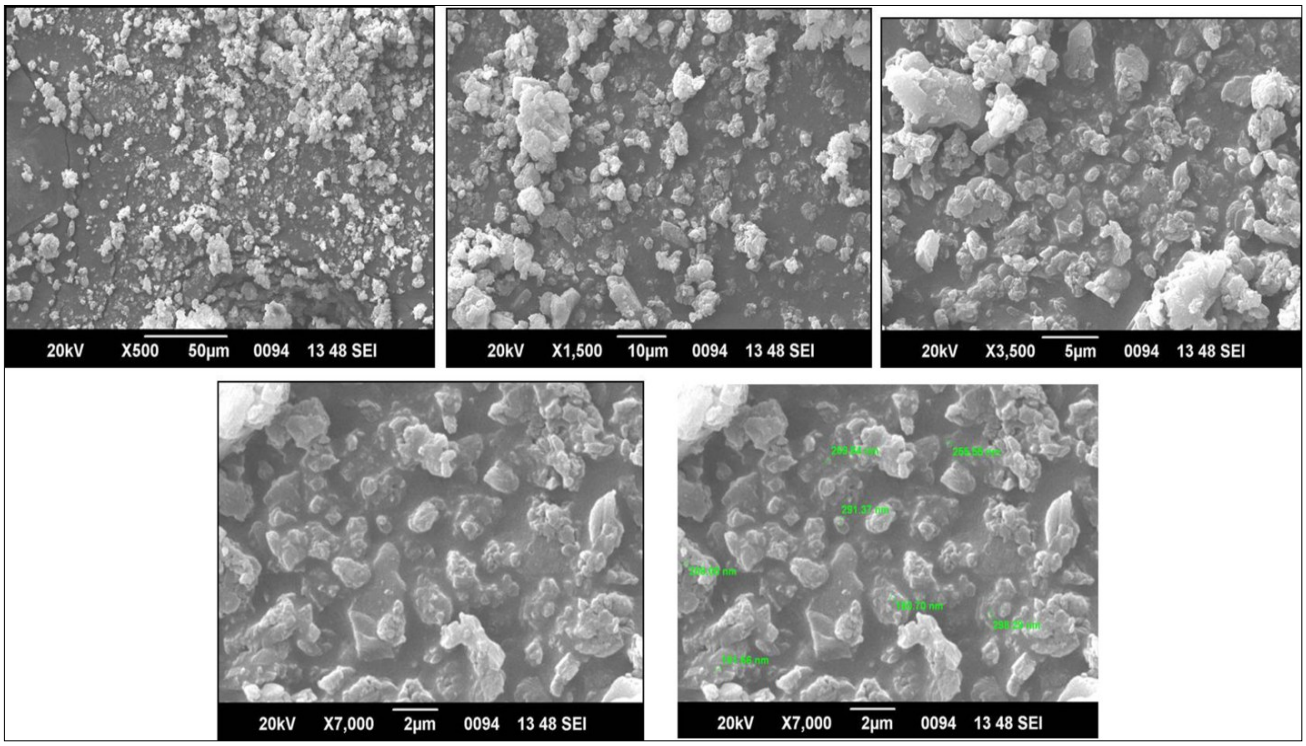

Fig. 5. Scanning electron microscopy at different scale of *Terminalia chebula* Soxhlet extract mediated zinc nanoparticles (TCZnS).

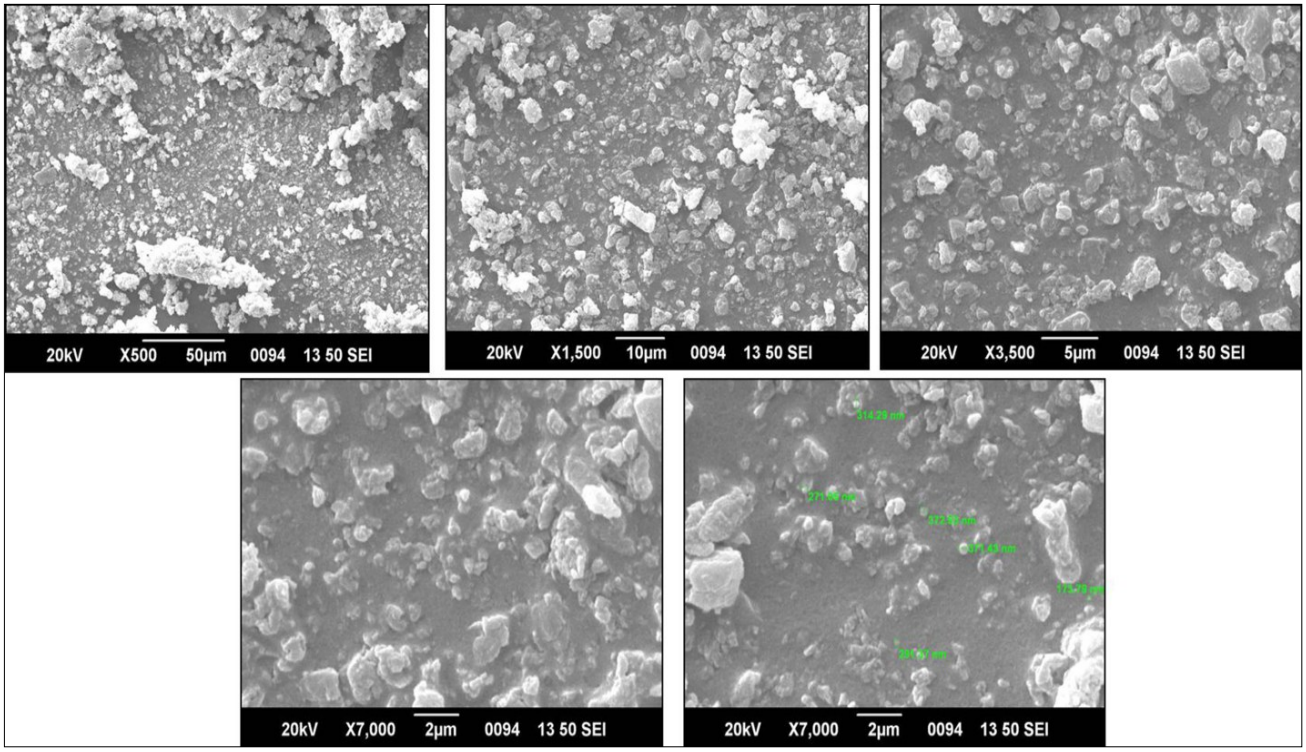

Fig. 6. Scanning electron microscopy at different scale of *Terminalia chebula* cold extract mediated zinc nanoparticles (TCZnC).

clusters rather than uniform spheres. The particles are not uniformly dispersed and show a clear tendency to aggregate, leading to a rough and heterogeneous surface. Qualitatively, particle sizes range from larger aggregates visible at lower magnifications (50 µm scale) down to individual nanoparticles or small clusters in the nanometer to sub-micron range at the highest magnification (2 µm scale). Researchers also showed that Zn Nanoparticles tend to agglomerate into larger particles due to their high surface area and surface energy (27).

Antimicrobial activity

In this study the antimicrobial properties of *T. chebula* extract, specifically its ZnNPs derived from Soxhlet and cold extraction methods, were tested by well diffusion method in concentration ranging from 50 to 250 µg/mL against *Escherichia coli, Staphylococcus pyogenes, Pseudomonas aeruginosa and Xanthomonas oryzae*. The effectiveness was measured by the zone of inhibition (ZOI), with streptomycin as a positive control and methanol as a negative control (Fig. 7, Table 1–4).

Overall, both synthesized nanoparticles showed potent antimicrobial activity that generally outperformed or matched streptomycin, while the negative control showed minimal or no inhibition. The study observed a concentration-dependent increase in activity up to 200 µg/mL for most strains, with a slight decrease at 250 µg/mL.

Nanoparticles synthesized from the Soxhlet extract of *T. chebula* (TCZnS) showed highest antimicrobial activity against *S. pyogenes*, reaching an impressive 35.3 ± 0.60 mm ZOI (Zone of inhibition) at a concentration of 200 µg/mL. This suggests ZnNPs synthesized from Soxhlet extract of *T. chebula* are particularly

Table 1. Antimicrobial activity of *Terminalia chebula* mediated ZnNPs against *Escherichia coli*

Concentration in µg/mL	Zone of inhibition in mm ± SE		
	TCZnS	TCZnC	PC
50	24 ± 0.5	20 ± 0	16.6 ± 0.6
100	23.6 ± 0.8	25 ± 0	14 ± 2
150	27.33 ± 0.6	31 ± 0.5	16 ± 1
200	22.6 ± 0.6	24.6 ± 0.3	16 ± 1
250	15.33 ± 0.3	17.33 ± 0.6	9.33 ± 0.6

TCZnS: *Terminalia chebula* Soxhlet extract mediated zinc nanoparticles; TCZnC: *Terminalia chebula* cold extract mediated zinc nanoparticles; PC: positive control. Treatment - p <0.001 (highly significant), concentration - p <0.05.

Table 2. Antimicrobial activity of *Terminalia chebula* mediated zinc nanoparticles against *Pseudomonas aeruginosa*

Concentration in µg/mL	Zone of inhibition in mm ± SE		
	TCZnS	TCZnC	PC
50	25 ± 0.50	27.6 ± 0.30	18.6 ± 0.30
100	34.6 ± 0.30	27 ± 0.50	16.6 ± 1.20
150	24 ± 0.50	26 ± 0.00	15.3 ± 1.30
200	28 ± 0.00	30.6 ± 0.60	16.3 ± 1.30
250	27 ± 1.10	15.6 ± 0.30	8.3 ± 1.60

TCZnS: *Terminalia chebula* Soxhlet extract mediated zinc nanoparticles; TCZnC: *Terminalia chebula* cold extract mediated zinc nanoparticles; PC: positive control. Treatment - p <0.001 (highly significant), concentration - not significant.

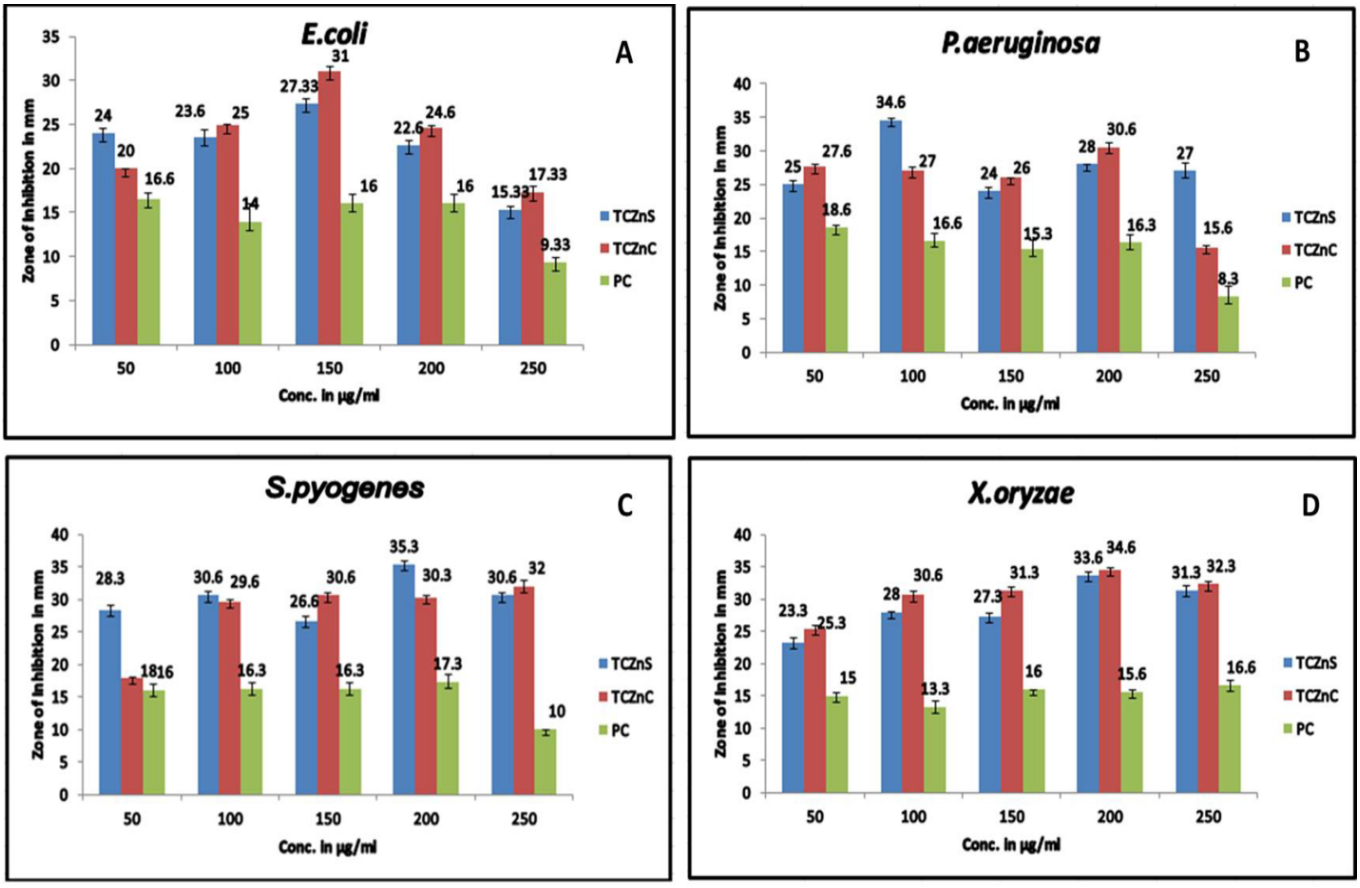

Fig. 7. Antimicrobial activity against; A: *Escherichia coli*; B: *Pseudomonas aeruginosa*; C: *Staphylococcus pyogenes*; D: *Xanthomonas oryzae* via. well diffusion method of *Terminalia chebula* fruit mediated zinc nanoparticles. TCZnS: *Terminalia chebula* Soxhlet extract mediated zinc nanoparticles; TCZnC: *Terminalia chebula* cold extract mediated zinc nanoparticles; PC: positive control.

Table 3. Antimicrobial activity of *Terminalia chebula* mediated zinc nanoparticles against *Staphylococcus pyogenes*

Concentration in µg/mL	Zone of inhibition in mm ± SE		
	TCZnS	TCZnC	PC
50	28.3 ± 0.80	18 ± 0.00	16 ± 1.00
100	30.6 ± 0.60	29.6 ± 0.30	16.3 ± 0.80
150	26.6 ± 0.80	30.6 ± 0.30	16.3 ± 0.80
200	35.3 ± 0.60	30.3 ± 0.30	17.3 ± 1.20
250	30.6 ± 0.30	32 ± 1.00	10 ± 0.00

TCZnS: *Terminalia chebula* Soxhlet extract mediated zinc nanoparticles; TCZnC: *Terminalia chebula* cold extract mediated zinc nanoparticles; PC: positive control. Treatment - p <0.001 (highly significant), concentration - not significant.

Table 4. Antimicrobial activity of *Terminalia chebula* mediated zinc nanoparticles against *Xanthomonas oryzae*

Concentration in µg/mL	Zone of inhibition in mm ± SE		
	TCZnS	TCZnC	PC
50	23.3 ± 0.60	25.3 ± 0.60	15 ± 0.50
100	28 ± 0.00	30.6 ± 0.60	13.3 ± 0.80
150	27.3 ± 0.60	31.3 ± 0.60	16 ± 0.00
200	33.6 ± 0.60	34.6 ± 0.30	15.6 ± 0.30
250	31.3 ± 0.80	32.3 ± 0.30	16.6 ± 0.80

TCZnS: *Terminalia chebula* Soxhlet extract mediated zinc nanoparticles; TCZnC: *Terminalia chebula* cold extract mediated zinc nanoparticles; PC: positive control. Treatment - p <0.001 (highly significant), concentration - p <0.05.

effective against this bacterium. For *P. aeruginosa*, the maximum zone of inhibition was 34.6 ± 0.30 mm at a slightly lower concentration of 100 µg/mL. Against *X. Oryzae*, the maximum ZOI was 33.6 ± 0.60 mm at 200 µg/mL, while *E. coli* showed a maximum activity of 27.33 ± 0.6 mm at 150 µg/mL.

Nanoparticles synthesized from the cold extract of *T. chebula* (TCZnC) also yielded significant antimicrobial activity. It demonstrated its strongest performance against *X. Oryzae*, achieving a highest ZOI of 34.6 ± 0.30 mm at 200 µg/mL. For *E. coli*, TCAgC proved slightly more effective than TCAgS, reaching 31 ± 0.5 mm ZOI at150 µg/mL. Against *S. pyogenes*, the maximum inhibition was 32 ± 1.00 mm at 250 µg/mL and for *P. aeruginosa*, the highest ZOI recorded was 30.6 ± 0.60 mm at 200 µg/mL. Both TCZnS and TCZnC along with positive control showed significant changes (p < 0.001) in zone of inhibition among the treatment group.

While both TCZnS and TCZnC were effective, TCZnC appeared slightly more effective for *E. coli* and *X. Oryzae* at higher concentrations, while TCZnS showed greater activity against *P. aeruginosa* at 100 µg/mL. For *S. pyogenes*, both TCZnS and TCZnC yielded comparable high activity.

In conclusion, *T. chebula* ZnNPs demonstrate broad-spectrum antimicrobial activity, often surpassing that of streptomycin. Optimal activity typically occurs between 150–200 µg/mL. The most significant inhibitions observed were 35.3 mm against *S. pyogenes* (TCZnS 200 µg/mL), 34.6 mm against *P. aeruginosa* (TCZnS 100 µg/mL) and 34.6 mm against *X. Oryzae* (TCZnC 200 µg/mL), highlighting *T. chebula*'s potential as a source for natural antimicrobial compounds. One study shows that the ZnNPs synthesized using cold *Aloe vera* extract exhibited significantly greater activity compared to particles derived from hot *A. vera* extract suggesting different method of extraction effects the phytochemical extracted and hence affecting its biological activities (28).

The decrease in antimicrobial activity at higher concentrations (250 µg/mL) can be attributed to several factors, such as saturation of bacterial cell membranes as high concentrations may saturate cell membranes, reducing effectiveness. Pro-oxidant effects, in which compounds may exhibit pro-oxidant properties at high concentrations, leading to oxidative stress and aggregation of compounds, they may aggregate, reducing surface area and interaction with bacteria (29, 30).

Conclusion

In conclusion the study successfully demonstrated the green synthesis of ZnNPs utilizing *T. chebula* fruit extract. The phytochemical richness of *T. chebula*, specifically its polyphenols, flavonoids and other compounds, proved instrumental in acting as both reducing and stabilizing agents during the nanoparticle formation. Comprehensive characterization using UV-Vis spectroscopy, FTIR, XRD and SEM confirmed the successful synthesis, crystalline nature (Average crystalline size of ~42–58 nm and ~15–32.8 nm for TCZnS and TCZnC respectively) and irregular morphology of the resulting ZnNPs.

Crucially, the synthesized *T. chebula* ZnNPs exhibited potent and broad-spectrum antimicrobial activity, often surpassing that of conventional antibiotics like streptomycin. This highlights the immense potential of biologically synthesized nanoparticles for developing effective and safer antimicrobial agents. The findings underscore the promise of integrating traditional medicinal plants with advanced nanotechnology, paving the way for innovative solutions in medicine, environmental remediation and sustainable materials science.

Acknowledgements

The authors express their sincere gratitude to the Department of Biotechnology, Guru Ghasidas Vishwavidyalaya (GGV), Bilaspur, Chhattisgarh, for providing the facilities required to carry out FTIR assays. The authors also gratefully acknowledge the Sophisticated Test and Instrumentation Centre (STIC), Cochin, for extending technical support in SEM and XRD analyses. The authors further acknowledge Indira Gandhi Krishi Vishwavidyalaya (IGKV), Raipur, Chhattisgarh, for providing the bacterial strain of *Xanthomonas oryzae*. The authors also acknowledge the support and facilities provided by D.L.S. P.G. College, Bilaspur, Chhattisgarh, the research centre where the study was conducted.

Authors' contributions

AS contributed to conceptualization, methodology and writing of the original draft. RP and NB contributed to supervision, review and editing of the manuscript. All authors read and approved the final manuscript.

Compliance with ethical standards

Conflict of interest: Authors do not have any conflict of interest to declare.

Ethical issues: None

Declaration of generative AI and AI-assisted technologies in the writing process

The authors declare that artificial intelligence (AI) tools such as Chat GPT, Quillbot were used only for language editing, grammar correction and improvement of readability of the manuscript. The scientific content, data interpretation, results and conclusions were entirely generated by the authors. The authors take full responsibility for the originality, accuracy and integrity of the work.

References

1. Sabir S, Arshad M, Chaudhari SK. Zinc oxide nanoparticles for revolutionizing agriculture: synthesis and applications. Sci World J. 2014;2014:1-8. https://doi.org/10.1155/2014/925494
2. Agarwal H, Kumar SV, Rajeshkumar S. A review on green synthesis of zinc oxide nanoparticles-an eco-friendly approach. Resour Effic Technol. 2017;3(4):406-13. https://doi.org/10.1016/j.reffit.2017.03.002
3. Munusamy T, Shanmugam R. Green synthesis of copper oxide nanoparticles synthesized by Terminalia chebula dried fruit extract: characterization and antibacterial action. Cureus. 2023;15 (12):e50142. https://doi.org/10.7759/cureus.50142
4. Barzinjy AA, Azeez HH. Green synthesis and characterization of zinc oxide nanoparticles using Eucalyptus globulus Labill. leaf extract and zinc nitrate hexahydrate salt. SN Appl Sci. 2020;2(5). https://doi.org/10.1007/s42452-020-2813-1
5. Sandar M, Sein NN, Win T. Biosynthesis of zinc oxide nanoparticles using fruit and leaf extracts of Terminalia chebula Retz. J Myanmar Acad Arts Sci. 2020;18(1).
6. Akhter SM, Siddiqui VU, Ahmad S, Husain D, Naeem S, Alam MT. Sustainable synthesis of zinc oxide nanoparticles using Terminalia chebula extract: effect of concentration and temperature on properties and antibacterial efficacy. Nano-Struct Nano-Objects. 2024;38:101158. https://doi.org/10.1016/j.nanoso.2024.101158
7. Sander LC. Soxhlet extractions. J Res Natl Inst Stand Technol. 2017;122:1. https://doi.org/10.6028/jres.122.001
8. Purena R, Bhatt R. Comparative phytochemical investigation, antioxidant and anticancer properties of leaf extracts of four medicinal plants from Chhattisgarh, India. Asian J Plant Sci Res. 2018;8(3):1-21.
9. Khandelwal KR. Practical pharmacognosy: techniques and experiments. 12th ed. Pune: Nirali Prakashan; 2004. p. 149-56.
10. Baranitharan M, Alarifi S, Alkahtani S, Ali D, Elumalai K, Pandiyan J, et al. Phytochemical analysis and fabrication of silver nanoparticles using Acacia catechu: an efficacious and eco-friendly control tool against selected polyphagous insect pests. Saudi J Biol Sci. 2020;28 (1):148-56. https://doi.org/10.1016/j.sjbs.2020.09.024
11. Ramesh P, Rajendran A, Meenakshisundaram M. Green synthesis of zinc oxide nanoparticles using flower extract Cassia auriculata. J Nanosci Nanotechnol. 2014;1:41-5.
12. Jayachandran AJ, TR A, Nair AS. Green synthesis and characterization of zinc oxide nanoparticles using Cayratia pedata leaf extract. Biochem Biophys Rep. 2021;26:100995. https://doi.org/10.1016/j.bbrep.2021.100995
13. Mohammadi FM, Ghasemi N. Influence of temperature and concentration on biosynthesis and characterization of zinc oxide nanoparticles using cherry extract. J Nanostruct Chem. 2018;8(1):93 -102. https://doi.org/10.1007/s40097-018-0257-6
14. Chennaiah MB, Kumar KD, Kumar BS, Tanneeru SR. Characterisation of zinc oxide nanoparticles-herbal synthesised coated with Ocimum tenuiflorum. Adv Mater Process Technol. 2021;8(Suppl 2):466-77. https://doi.org/10.1080/2374068X.2021.1934642
15. Pillai AM, Sivasankarapillai VS, Rahdar A, Joseph J, Sadeghfar F, A RA, et al. Green synthesis and characterization of zinc oxide nanoparticles with antibacterial and antifungal activity. J Mol Struct. 2020;1211:128107. https://doi.org/10.1016/j.molstruc.2020.128107
16. Akhter SMH, Mohammad F, Ahmad S. Terminalia belerica mediated green synthesis of nanoparticles of copper, iron and zinc metal oxides as the alternate antibacterial agents against some common pathogens. Bio NanoScience. 2019;9(2):365-72. https://doi.org/10.1007/s12668-019-0601-4
17. Adam OA, Abadi RS, Ayoub SM. The effect of extraction method and solvents on yield and antioxidant activity of certain Sudanese medicinal plant extracts. J Phytopharmacol. 2019;8(5):248-52. https://doi.org/10.31254/phyto.2019.8507
18. Kumar SS, Venkateswarlu P, Rao VR, Rao GN. Synthesis, characterization and optical properties of zinc oxide nanoparticles. Int Nano Lett. 2013;3(1). https://doi.org/10.1186/2228-5326-3-30
19. Shamhari NM, Wee BS, Chin SF, Kok KY. Synthesis and characterization of zinc oxide nanoparticles with small particle size distribution. Acta Chim Slov. 2018;65(3):578-85.https://doi.org/10.17344/acsi.2018.4213
20. Talam S, Karumuri SR, Gunnam N. Synthesis, characterization and spectroscopic properties of ZnO nanoparticles. ISRN Nanotechnol. 2012;2012:1-6. https://doi.org/10.5402/2012/372505
21. Saha R, Karthik S, Balu KS, Suriyaprabha R, Siva P, Rajendran V. Influence of the various synthesis methods on the ZnO nanoparticles property made using the bark extract of Terminalia arjuna. Mater Chem Phys. 2018;209:208-16. https://doi.org/10.1016/j.matchemphys.2018.01.023
22. Congyang M, Xiang Y, Liu X, Cui Z, Yang X, Yeung KWK, et al. Photo-inspired antibacterial activity and wound healing acceleration by hydrogel embedded with Ag/Ag@AgCl/ZnO nanostructures. ACS Nano. 2017;11:9010-21. https://doi.org/10.1021/acsnano.7b03513
23. Alahmdi MI, Khasim S, Vanaraj S, Panneerselvam C, Mahmoud MA, Mukhtar S, et al. Green nanoarchitectonics of ZnO nanoparticles from Clitoria ternatea flower extract for in vitro anticancer and antibacterial activity: inhibits MCF-7 cell proliferation via intrinsic apoptotic pathway. J Inorg Organomet Polym Mater. 2022;32 (6):2146-59. https://doi.org/10.1007/s10904-022-02263-7
24. Somu P, Khanal HD, Gomez LA, Shim JJ, Lee YR. Multifunctional biogenic Al-doped zinc oxide nanostructures synthesized using bioreductant Chaetomorpha linum extract exhibit excellent photocatalytic and bactericidal ability in industrial effluent treatment. Biomass Convers Biorefin. 2025;15:22025-40. https://doi.org/10.1007/s13399-022-03177-7
25. Zhou XQ, Hayat Z, Zhang DD, Li MY, Hu S, Wu Q, et al. Zinc oxide nanoparticles: synthesis, characterization, modification and applications in food and agriculture. Processes. 2023;11(4):1193. https://doi.org/10.3390/pr11041193
26. Liou TH, Wang SY, Lin YT, Yang S. Sustainable utilization of rice husk waste for preparation of ordered nanostructured mesoporous silica and mesoporous carbon: characterization and adsorption performance. Colloids Surf A Physicochem Eng Asp. 2022;636:128150. https://doi.org/10.1016/j.colsurfa.2021.128150
27. Srivastava V, Gusain D, Sharma YC. Synthesis, characterization and application of zinc oxide nanoparticles (n-ZnO). Ceram Int. 2013;39 (8):9803-08. https://doi.org/10.1016/j.ceramint.2013.04.110
28. Venkataraju JL, Sharath R, Chandraprabha MN, Neelufar E, Hazra A, Patra M. Synthesis, characterization and evaluation of antimicrobial activity of zinc oxide nanoparticles. J Biochem Technol. 2014;3

(5):151-4.

29. Gebremichael TE, Tesfaye E, Abebe T, Bekele A, Robi ZH, Gebremikael TE. Bio-derived NiO nanoparticles from Colocasia esculenta leaf extract with enhanced antibacterial activity and efficient photocatalytic degradation of methylene blue. RSC Adv. 2026;16(3):2030-43. https://doi.org/10.1039/D5RA08840B

30. Joseph CO. Phytochemical profiling and bioactivity assessment of the ethanol extract of Lannea schimperi bark: antioxidant, antiradical and antimicrobial potentials. BMC Complement Med Ther. 2026. https://doi.org/10.1186/s12906-025-05219-9

Additional information

Peer review: Publisher thanks Sectional Editor and the other anonymous reviewers for their contribution to the peer review of this work.

Reprints & permissions information is available at https://horizonepublishing.com/journals/index.php/PST/open_access_policy

Publisher's Note: Horizon e-Publishing Group remains neutral with regard to jurisdictional claims in published maps and institutional affiliations.

Indexing: Plant Science Today, published by Horizon e-Publishing Group, is covered by Scopus, Web of Science, BIOSIS Previews, Clarivate Analytics, NAAS, UGC Care, etc
See https://horizonepublishing.com/journals/index.php/PST/indexing_abstracting

Publisher information: Plant Science Today is published by HORIZON e-Publishing Group with support from Empirion Publishers Private Limited, Thiruvananthapuram, India.